

Charge-Localizing Effect in Alkali-Metal Enolates and Phenolates. Structure and Aromaticity of the Phenolate Anion

Thomas Kremer and Paul von Ragué Schleyer*

Institut für Organische Chemie der Friedrich Alexander Universität Erlangen-Nürnberg,
Henkestrasse 42, D-91054 Erlangen, Germany

Received September 4, 1996[®]

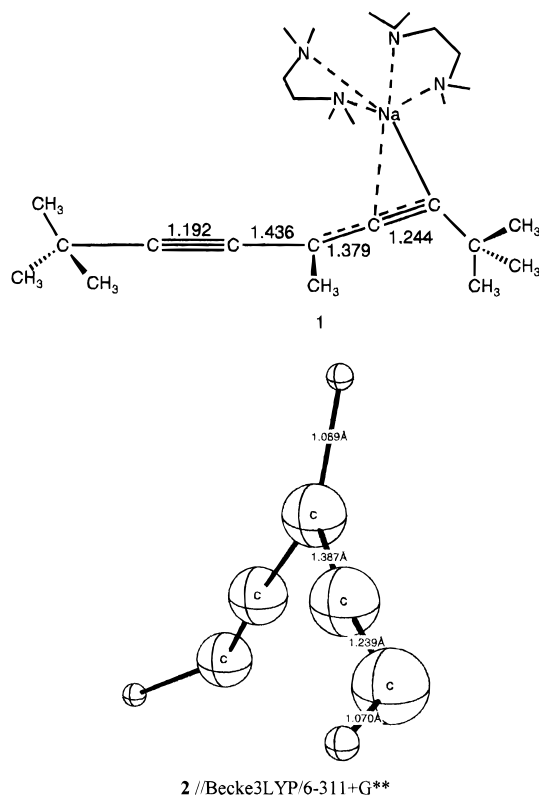
Alkali-metal counterion interactions influence the enolate and phenolate anions considerably. Like the acetaldehyde enolate anion, the stabilization energies of the phenolate anion (vs OH⁻) are very much reduced in the corresponding alkali-metal ion pairs. The stabilization energies (relative to OH⁻) of 34.9 kcal/mol for the free enolate anion and 40.9 kcal/mol for the phenolate ion (computed with the Becke3LYP density functional on the MP2(full)/6-31+G* optimized structures) reproduce the experimental gas-phase data well. The metal gegenion induced negative charge *localization* on the enolate and phenolate oxygens varies only somewhat along the Li–Cs series but reduces the stabilization energies enormously: for the enolates to 8–14 kcal/mol and to 9–15 kcal/mol for the phenolates (vs MOH). These ion pair interactions influence the geometries, the charge distributions, the ¹³C chemical shifts, and the reaction energies of alkali-metal enolates and phenolates but do so to similar extents in both systems. Charge localization is still effective at long metal–oxygen distances, since electrostatic interaction energies decrease only with the inverse of the distance. The phenolate anion has considerable quinoid character, and judging from the geometry and the magnetic criteria (NICS and Λ , the magnetic susceptibility exaltation) its aromaticity is reduced to about 60% of that of phenol and the alkali-metal ion-paired phenolates.

Introduction

The structures, energies, reactivities, and the mechanisms of polar organometallic compounds are strongly influenced by the metal gegenion.^{1,2} While π -delocalization, negative hyperconjugation, polarization, and inductive effects are greatest in free carbanions,² the electrostatic stabilization of the anion by the metal counterion, as well as solvation and the degree of aggregation, may determine the structure and stability of polar organometallic compounds in condensed phases. The largely electrostatic interactions with the cation compete with other modes of stabilization of the anion, e.g. π - and σ -delocalization. The charge localization due to the electrostatic interaction with the counterion influences the structure, energy, and behavior of this ion pair relative to the free anion considerably.^{2–6}

The charge localizing effect of the alkali-metal gegenion was first demonstrated computationally by Schleyer and co-workers.³ An intriguing example is the unsymmetrical X-ray structure of 3-[bis(tetramethyl-ethylendiamino)sodio]-2,2,5,8,8-pentamethyl-nona-3,4-

dien-6-yne (1).^{4a} While parent free carbanion (2), sta-



bilized by electron delocalization, is computed to be

(4) (a) Schade, C.; Schleyer, P. v. R.; Geissler, M.; Weiss, E. *Angew. Chem., Int. Ed. Engl.* **1986**, *25*, 902. (b) Dem'yanov, P.; Boche, G.; Marsch, M.; Harms, K.; Fyodorova, G.; Petrosyan, V. *Liebigs Ann.* **1995**, 457.

[®] Abstract published in *Advance ACS Abstracts*, January 15, 1997.

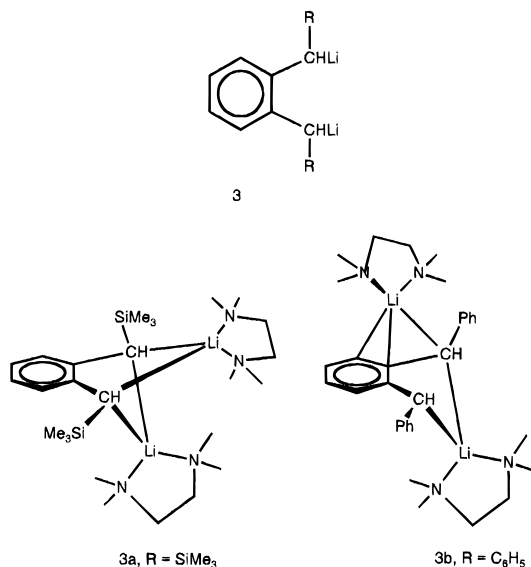
(1) Schlosser, M. In *Strukturen und Reaktivität polarer Organometalle*; Springer: Berlin, 1973.

(2) (a) Lambert, C.; Schleyer, P. v. R. In *Methoden der organischen Chemie (Houben-Weyl)*; Georg Thieme Verlag: Stuttgart, Germany, 1993; Bd. E19d (Carbanionen). (b) Lambert, C.; Schleyer, P. v. R. *Angew. Chem., Int. Ed. Engl.* **1994**, *33*, 1129. (c) Schleyer, P. v. R. *Pure Appl. Chem.* **1983**, *55*, 355. (d) Schleyer, P. v. R. *Pure Appl. Chem.* **1984**, *56*, 151. (e) Setzer, W. N.; Schleyer, P. v. R. *Adv. Organomet. Chem.* **1985**, *24*, 353. (f) Schade, C.; Schleyer, P. v. R. *Adv. Organomet. Chem.* **1987**, *27*, 169. (g) Boche, G. *Angew. Chem., Int. Ed. Engl.* **1989**, *28*, 277. (h) Weiss, E. *Angew. Chem., Int. Ed. Engl.* **1993**, *32*, 1501. (i) Bock, H.; Näther, C.; Havlas, Z.; John, A.; Arad, C. *Angew. Chem., Int. Ed. Engl.* **1994**, *33*, 1129.

(3) Schleyer, P. v. R.; Chandrasekhar, S.; Kos, A. J.; Clark, T.; Spitznagel, G. W. *J. Chem. Soc., Chem. Commun.* **1981**, 882.

symmetrical, the off-center sodium ion placement in **1** results in an unsymmetrical carbon skeleton topology.⁴ Consequently the resonance stabilization of the free anion **2** (which has two essentially equal-energy isomers with C_s and C_2 symmetry) is reduced considerably in the ion pair. The electrostatic interaction with the cation results in a more localized charge distribution in the anion.

Another early example of charge localization was provided by comparisons of the X-ray structures of two differently-substituted dilithiated *ortho*-xylenes (**3a, b**).^{2e,5}



The parent dianions of both are symmetrical. While both lithium atoms in **3a** (R = SiMe₃)^{5a} bridge the two benzylic carbon atoms, **3b** (R = C₆H₅)^{5b} is unsymmetrical; only one lithium bridges the benzylic carbons, and the other one bridges a benzylic carbon and the C(3) ring carbon. The differences in the bridging modes were interpreted electrostatically: trimethylsilyl groups stabilize carbanions very effectively,⁶ predominantly by polarization and negative hyperconjugation,^{6a} and tend to *localize* the negative charge of **3a** at the benzylic carbons. The positive charged lithium atoms bridge symmetrically between these centers of highest negative charge. The phenyl substituents in **3b** *delocalize* the negative charge away from the benzylic carbons. Hence, the second lithium cation does not bridge as in **3a** but interacts with another region of high electron density, namely the benzylically delocalized negative charge in the *ortho*-xylene ring.

Enolates and phenolates of the alkali metals provide additional demonstrations of the localizing effect of ion pairing. Lambert, Wu, and Schleyer's pseudopotential study found that the stabilization of the free enolate anion (ca. 33 kcal/mol vs OH⁻) is drastically reduced to 9–14 kcal/mol (vs MOH) in the ion paired alkali enolates.^{7a} Enolates or phenolates with different alkali-metal counterions show varying reactivity, which has

(5) (a) Lappert, M. F.; Raston, C. L.; Skelton, B. W.; White, A. J. *J. Chem. Soc., Chem. Commun.* **1984**, 14. (b) Boche, G.; Decher, G.; Etzrodt, H.; Dietrich, H.; Mahdi, W.; Kos, A. J.; Schleyer, P. v. R. *J. Chem. Soc., Chem. Commun.* **1984**, 1493.

(6) (a) Schleyer, P. v. R.; Clark, T.; Kos, A. J.; Spitznagel, G. W.; Rohde, C.; Arad, D.; Houk, K. N.; Rondan, N. G. *J. Am. Chem. Soc.* **1984**, *106*, 6467. (b) Schleyer, P. v. R.; Jemmis, D. E.; Spitznagel, G. W. *J. Am. Chem. Soc.* **1985**, *107*, 6393. (c) Schleyer, P. v. R. *Pure Appl. Chem.* **1987**, *59*, 1647.

been attributed to the structural changes (also the extent of aggregation) due to the metal.⁸ The Kolbe–Schmitt reaction is a textbook example: sodium phenoxide is carboxylated by carbon dioxide mostly in the *ortho* position, whereas carboxylation of potassium phenoxide gives the *para* product predominantly.⁹

Polar organometallic compounds are studied *inter alia* by NMR spectroscopy¹⁰ and by colligative measurements in solution.¹¹ For carbon-bound organometallics, ⁶Li, ¹³C coupling can reveal the degree of aggregation; the same is true for the ⁶Li, ¹⁵N coupling in lithium amides.¹² Jackman *et al.* used ⁷Li quadrupole splitting constants (QSC), which are a function of the electrical environment of the Li nucleus (and hence of the aggregation size), to elucidate the structure of organolithium derivatives in solution.¹³ Jackman also employed lithium phenolates as model enolates.¹³

Although many X-ray structures of phenolates^{15,16} and

(7) (a) Lambert, C.; Wu, Y.-D.; Schleyer, P. v. R. *J. Chem. Soc., Chem. Commun.* **1993**, 255. (b) Lynch, T. J.; Newcomb, M.; Bergbreiter, D. E.; Hall, M. B. *J. Org. Chem.* **1980**, *45*, 5005. (c) For earlier data, see ref 7b and references cited.

(8) (a) Seebach, D. *Angew. Chem., Int. Ed. Engl.* **1988**, *27*, 1685 and references cited. (b) Heathcock, C. H. In *Modern Synthetic Methods*; Scheffold, R., Ed.; Verlag Helv. Chim. Acta and VCH Verlagsges.: Basel, Weinheim, 1992; Bd. 6, S.1. (c) Evans, D. A. In *Asymmetric Synthesis*; Morrison, J. D., Ed.; Academic Press: New York, 1984; Vol. 3, Part B, pp 2–110. (d) Heathcock, C. H. In *Asymmetric Synthesis*; Morrison, J. D., Ed.; Academic Press: New York, 1984; Vol. 3, Part B, pp 111–212. (e) Kaufman, M. J.; Gronert, S. V.; Bors, D. A.; Streitwieser, A. *J. Am. Chem. Soc.* **1987**, *109*, 602. (f) Ciula, J. C.; Streitwieser, A. *J. Org. Chem.* **1992**, *57*, 431.

(9) March, J. *Advanced Organic Chemistry*; Wiley-Interscience: New York, 1992; pp 546–547.

(10) (a) Fraenkel, G.; Fraenkel, A. M.; Geckle, M. J.; Schloss, F. J. *Am. Chem. Soc.* **1979**, *101*, 4745. (b) Seebach, D.; Hässig, R.; Gabriel, J. *Helv. Chim. Acta* **1983**, *66*, 308. (c) Bauer, W.; Schleyer, P. v. R. In *Advances in Carbanion Chemistry*; Snieckus, V., Ed.; Jai Press: London, 1992; Vol. 1, pp 89–175. (d) Bauer, W. In *Lithium Chemistry*; Sapse, A. M.; Schleyer, P. v. R., Eds.; Wiley Interscience: New York, 1995; pp 125–172.

(11) (a) Bauer, W.; Seebach, D. *Helv. Chim. Acta* **1984**, *67*, 1972. (12) (a) Kallman, N.; Collum, D. B. *J. Am. Chem. Soc.* **1987**, *109*, 7466. (b) Galiano-Roth, A. S.; Michaelides, E. M.; Collum, D. B. *J. Am. Chem. Soc.* **1988**, *110*, 2658. (c) Jackman, L. M.; Scarmoutzos, L. M.; Porter, W. *J. Am. Chem. Soc.* **1987**, *109*, 6524. (d) Jackman, L. M.; Scarmoutzos, L. M. *J. Am. Chem. Soc.* **1987**, *109*, 5348. (e) Jackman, L. M.; Scarmoutzos, L. M.; Smith, B. D.; Williard, P. G. *J. Am. Chem. Soc.* **1987**, *109*, 6058. (f) Galiano-Roth, A. S.; Collum, D. B. *J. Am. Chem. Soc.* **1989**, *111*, 6772. (g) Gilchrist, J. H.; Harrison, A. T.; Fuller, D. J.; Collum, D. B. *J. Am. Chem. Soc.* **1990**, *112*, 4069. (h) Hall, P. L.; Gilchrist, J. H.; Harrison, A. T.; Fuller, D. J.; Collum, D. B. *J. Am. Chem. Soc.* **1991**, *113*, 9575. (i) Romesberg, F. E.; Gilchrist, J. H.; Harrison, A. T.; Fuller, D. J.; Collum, D. B. *J. Am. Chem. Soc.* **1991**, *113*, 5751.

(13) (a) Jackman, L. M.; Lange, B. C. *Tetrahedron* **1977**, *33*, 2737. (b) Jackman, L. M.; DeBrosse, C. W. *J. Am. Chem. Soc.* **1983**, *105*, 4177. (c) Jackman, L. M.; Scarmoutzos, L. M.; DeBrosse, C. W. *J. Am. Chem. Soc.* **1987**, *109*, 5355. (d) Jackman, L. M.; Smith, B. D. *J. Am. Chem. Soc.* **1988**, *110*, 3829. (e) Jackman, L. M.; Rakiewicz, E. F.; Benesi, A. J. *J. Am. Chem. Soc.* **1991**, *113*, 4041. (f) Jackman, L. M.; Petrei, M. M.; Smith, B. D. *J. Am. Chem. Soc.* **1991**, *113*, 3451. (g) Jackman, L. M.; Chen, X. *J. Am. Chem. Soc.* **1992**, *114*, 403. (h) Jackman, L. M.; Çizmeçiyen, D.; Williard, P. G.; Nichols, M. A. *J. Am. Chem. Soc.* **1993**, *115*, 6262.

(14) (a) Amstutz, R.; Schweizer, W. B.; Seebach, D.; Dunitz, J. D. *Helv. Chim. Acta* **1981**, *64*, 2617. (b) Bauer, W.; Laube, T.; Seebach, D. *Chem. Ber.* **1985**, *118*, 764. (c) Williard, P. G.; Carpenter, G. B. *J. Am. Chem. Soc.* **1985**, *107*, 3345. (d) Laube, T.; Dunitz, J. D.; Seebach, D. *Helv. Chim. Acta* **1985**, *68*, 1373. (e) Williard, P. G.; Carpenter, G. B. *J. Am. Chem. Soc.* **1986**, *108*, 462. (f) Williard, P. G.; Mac Ewan, G. J. *J. Am. Chem. Soc.* **1989**, *111*, 7671. (g) Hahn, E.; Maetzke, T.; Plattner, D. A.; Seebach, D. *Chem. Ber.* **1990**, *123*, 2059. (h) Gomez-Sanchez, A.; Lassaletta, J.-M.; Lopez-Castro, A.; Dianez, M. J.; Estrada, M. D.; Perez-Garrido, S. *Tetrahedron Lett.* **1992**, *33*, 1361. (i) Williard, P. G.; Liu, Q.-Y. *J. Am. Chem. Soc.* **1993**, *115*, 3380. (j) Henderson, K. W.; Williard, P. G.; Bernstein, P. R. *Angew. Chem., Int. Ed. Engl.* **1995**, *34*, 1117.

(15) (a) Malhorta, K. C.; Martin, R. L. *J. Organomet. Chem.* **1982**, *239*, 159. (b) Pauer, F.; Power, P. P. In *Lithium Chemistry*; Sapse, A. M., Schleyer, P. v. R., Eds.; Wiley Interscience: New York, 1995; pp 295–392.

enolates¹⁴ have been reported, different degrees of aggregation and solvation prevent direct comparisons of the gegenion influences. *Ab initio* calculations¹⁷ obviate such experimental complications and can be expected to give reliable results.¹⁸ We now compare the ability of alkali-metal counterions to localize charge in enolates with the behavior in phenolates, e.g. with regard to the geometries and the charge distributions in both sets of species. We also have included bridged alkali enolates^{7b} in our study. To what extent do phenolates model enolates? Our prior work^{7a} on the charge-localizing effect in alkali enolates has been refined at more sophisticated levels of *ab initio* theory (HF, MP2, and Becke3LYP DFT), including electron correlation, for comparison with the new phenolate data.

Nucleus-independent chemical shifts (NICS),¹⁹ the negative of the absolute magnetic shieldings computed at ring centers (nonweighted mean of the heavy atom coordinates), have been introduced by Schleyer and co-workers as a simple aromaticity probe.^{19,20} To demonstrate the effect of charge localization on aromaticity as well as on chemical shifts, we have employed GIAO²¹-NMR NICS calculations, as well as evaluations of the magnetic susceptibility exaltations²² and anisotropies²³ (additional criteria of aromaticity),²⁰ on the MP2-optimized geometries.

(16) (a) van Beylen, M.; Roland, B.; King, G. S. D.; Aerts, J. *J. Chem. Res.* **1985**, 388, 4201. (b) Dougherty, S. M.; Stoddart, J. F.; Colquhoun, H. M.; Slawin, A. M. Z.; Williams, D. J. *Polyhedron* **1985**, 567. (c) Hundal, M. S.; Sood, G.; Kapoor, P.; Poonia, N. S. *J. Crystallogr. Spectrosc. Res.* **1991**, 21, 201. (d) Cetinkaya, B.; Gümrükçü, I.; Lappert, M. F.; Atwood, J. L.; Shakir, R. *J. Am. Chem. Soc.* **1980**, 102, 2086. (e) Huffman, J. C.; Geerts, R. L.; Caulton, K. G. *J. Crystallogr. Spectrosc.* **1984**, 14, 541. (f) Murchie, B.; Bovenkamp, J. W.; Rodrigue, A.; Watson, K. A.; Fortier, S. *Can. J. Chem.* **1988**, 66, 2515. (g) Watson, K. A.; Fortier, S.; Murchie, M. P.; Bovenkamp, J. W.; Rodrigue, A.; Buchanan, G. W.; Ratcliffe, C. J. *Can. J. Chem.* **1990**, 68, 1201. (h) Korobov, M. S.; Minkin, V. I.; Nivorozhkin, L. E.; Kompan, O. E.; Struchkov, Y. T. *Zh. Obshch. Khim.* **1989**, 59, 429. (i) van den Schaff, P. A.; Jastrzebski, J. T. B. H.; Hogenheide, M. P.; Smeets, W. J. J.; Spek, A. L.; Boersma, J.; van Koten, G. *Inorg. Chem.* **1993**, 32, 4111. (j) van den Schaff, P. A.; Hogenheide, M. P.; Grove, D.; Spek, A. L.; van Koten, G. *J. Chem. Soc., Chem. Commun.* **1992**, 1703.

(17) Hehre, W. J.; Radom, L.; Schleyer, P. v. R.; Pople, J. A. *Ab Initio Molecular Orbital Theory*; Wiley: New York, 1986.

(18) (a) Kaufmann, E.; Schleyer, P. v. R.; Houk, K. N.; Wu, Y.-D. *J. Am. Chem. Soc.* **1985**, 107, 5560. (b) McKee, M. L. *J. Am. Chem. Soc.* **1987**, 109, 559. (c) Kaufmann, E.; Schleyer, P. v. R.; Gronert, S.; Streitwieser, A.; Halpern, M. *J. Am. Chem. Soc.* **1987**, 109, 2553. (d) Kaufmann, E.; Schleyer, P. v. R. *J. Comput. Chem.* **1989**, 4, 437. (e) Li, Y.; Paddon-Row, M. N.; Houk, K. N. *J. Am. Chem. Soc.* **1988**, 110, 3684. (f) Kaufmann, E.; Sieber, S.; Schleyer, P. v. R. *J. Am. Chem. Soc.* **1989**, 111, 121. (g) Kaufmann, E.; Sieber, S.; Schleyer, P. v. R. *J. Am. Chem. Soc.* **1989**, 111, 4005. (h) Leung-Toung, R.; Tidwell, T. T. *J. Am. Chem. Soc.* **1990**, 112, 1042. (i) Li, Y.; Paddon-Row, M. N.; Houk, K. N. *J. Org. Chem.* **1990**, 55, 481. (j) van Eikema Hommes, N. J. R.; Bühl, M.; Schleyer, P. v. R.; Wu, Y.-D. *J. Organomet. Chem.* **1991**, 409, 307. (k) van Eikema Hommes, N. J. R.; Schleyer, P. v. R. *Angew. Chem., Int. Ed. Engl.* **1992**, 31, 755. (l) Lambert, C.; Kaupp, M.; Schleyer, P. v. R. *Organometallics* **1993**, 12, 853. (m) Kremer, T.; Harder, S.; Junge, M.; Schleyer, P. v. R. *Organometallics* **1996**, 15, 585.

(19) Schleyer, P. v. R.; Maerker, C.; Dransfeld, A.; Jiao, H.; van Eikema Hommes, N. J. R. *J. Am. Chem. Soc.* **1996**, 118, 6317. (b) Jiao, H.; Schleyer, P. v. R. *Angew. Chem.*, in press. (c) Govindan, S.; Schleyer, P. v. R.; Jiao, H. *Angew. Chem.*, in press.

(20) Schleyer, P. v. R.; Jiao, H. *Pure Appl. Chem.* **1996**, 68, 209.

(21) Wolinski, K.; Hinton, J. F.; Pulay, P. *J. Am. Chem. Soc.* **1990**, 112, 8251.

(22) (a) Dauben, H. J., Jr.; Wilson, J. D.; Laity, J. L. *J. Am. Chem. Soc.* **1968**, 90, 811. (b) Dauben, H. J., Jr.; Wilson, J. D.; Laity, J. L. *J. Am. Chem. Soc.* **1969**, 91, 1991. (c) Dauben, H. J., Jr.; Wilson, J. D.; Laity, J. L. *Nonbenzenoid Aromaticity*, Snyder, J. P., Ed.; Academic Press: New York, 1971; Vol. 2, pp 167–206.

(23) (a) Benson, R. C.; Flygare, W. H. *J. Am. Chem. Soc.* **1970**, 92, 7523. (b) Schmalz, T. G.; Norris, C. L.; Flygare, W. H. *J. Am. Chem. Soc.* **1973**, 95, 7961. (c) Schmalz, T. G.; Gierke, T. D.; Beak, P.; Flygare, W. H. *Tetrahedron Lett.* **1974**, 33, 2885. (d) Palmer, M. H.; Findlay, R. H. *Tetrahedron Lett.* **1974**, 33, 253. (e) Hutter, D. H.; Flygare, W. H. *Top. Curr. Chem.* **1976**, 63, 89.

Computational Methods

The use of pseudopotentials to replace core electrons diminishes the computational costs, compared to all-electron calculations, for compounds of the heavier elements K, Rb, and Cs considerably.^{24,25} In contrast to the lighter alkali metals, core polarizability is significant for the heavier alkali metals K–Cs. Hence, nine-valence electron (valence plus $n-1$ shell) effective core potentials (ECP) were employed for K, Rb, and Cs, as the implicit frozen-core approximation leads to large errors in one-valence electron ECP treatments.²⁶ General basis sets 6-31+G* (basis A) were used for Li, Na, H, C, and O. More flexible (21111/21111/11) valence basis sets, optimized with effective core potentials, including a double set of uncontracted d functions from Huzinaga *et al.* were used for the heavier alkali metals (K, Rb, Cs).²⁷ All geometries were optimized within the given symmetry at Hartree–Fock (RHF/basis A), correlated (MP2(full)/basis A), and density functional theory (DFT)²⁸ (Becke3LYP/basis A) levels using the gradient optimization techniques implemented in the Gaussian 92/DFT and Gaussian 94 program packages.²⁹ All stationary points were characterized to be true minima by frequency computations at the RHF/(basis A) level. Atomic charges and bond orders were calculated using the natural population (NPA) and natural bond orbital (NBO) analysis methods developed by Reed and Weinhold.³⁰ DFT single point calculations on the MP2(full)/basis A optimized structures, using the general 6-311++G** basis set for Li, Na, H, C, and O (basis B) and the (21111/21111/11) basis sets together with the pseudopotentials for K–Cs provide our highest level data; these are the energies discussed in the text (see Table 1 for details). The corrections for differences in zero point vibrational energy (at RHF/basis A) were scaled by 0.89.¹⁷ Total energies and zero point energies are given in Table 1. Diamagnetic susceptibilities and diamagnetic susceptibility anisotropies (Becke3LYP/6-31G*, using the CSGT (continuous set in gauge transformations) method)³¹ and nucleus-independent chemical shifts

(24) Szasz, L. *Pseudopotential Theory of Atoms and Molecules*; Wiley Interscience: New York, 1985.

(25) (a) Müller, W.; Meyer, W. *J. Chem. Phys.* **1984**, 80, 3311. (b) Fuentealba, P.; Reyes, O.; Stoll, H.; Preuss, H. *J. Chem. Phys.* **1987**, 87, 5338. (c) Langhoff, S. R.; Bauschlicher, C. W., Jr.; Partridge, H. *J. Chem. Phys.* **1986**, 85, 5158. (d) Langhoff, S. R.; Bauschlicher, C. W., Jr.; Partridge, H. *J. Chem. Phys.* **1986**, 84, 1687. (e) Bauschlicher, C. W., Jr.; Langhoff, S. R.; Partridge, H. *J. Chem. Phys.* **1986**, 84, 901.

(26) (a) Partridge, H.; Bauschlicher, C. W., Jr.; Walch, S. P.; Liu, B. *J. Chem. Phys.* **1983**, 79, 1866. (b) Müller, W.; Flesch, J.; Meyer, W. *J. Chem. Phys.* **1984**, 80, 3297. (c) Jeung, G.; Daudey, J.-P.; Malrieu, J.-P. *Chem. Phys. Lett.* **1983**, 98, 433. (d) Petterson, L. G. M.; Siegbahn, P. E. M.; Ismail, S. *Chem. Phys.* **1983**, 82, 355. (e) Kaupp, M.; Schleyer, P. v. R.; Stoll, H.; Preuss, H. *J. Chem. Phys.* **1991**, 94, 1360.

(27) (a) Kaupp, M.; Bergner, A.; Küchle, W.; Preuss, H.; Stoll, H. Unpublished results. (b) Huzinaga, S. *Gaussian Basis Sets for Molecular Calculations*; Elsevier: Amsterdam, 1984.

(28) (a) Ziegler, T. *Chem. Rev.* **1991**, 91, 651. (b) Becke, A. D. *J. Chem. Phys.* **1993**, 98, 5648. (c) Labanowski, J. W.; Andzelm, J. *Density Functional Methods in Chemistry*; Springer: New York, 1991. (d) Parr, R. G.; Yang, W. *Density Functional Theory of Atoms and Molecules*; Oxford University Press: New York, 1989. (e) Stephens, P. J.; Devlin, F. J.; Chabalowski, C. F.; Frisch, M. J. *J. Phys. Chem.* **1994**, 98, 11623.

(29) (a) Gaussian 92/DFT, Revision G.2: Frisch, M. J.; Trucks, G. W.; Schlegel, H. B.; Gill, P. M. W.; Johnson, B. G.; Wong, M. W.; Foresman, J. B.; Robb, M. A.; Head-Gordon, M.; Replogle, E. S.; Gomperts, R.; Andres, J. L.; Raghavachari, K.; Binkley, J. S.; Gonzalez, C.; Martin, R. L.; Fox, D. J.; Defrees, D. J.; Baker, J.; Stewart, J. J. P.; Pople, J. A. Gaussian, Inc., Pittsburgh, PA, 1993. (b) Gaussian 94: Frisch, M. J.; Trucks, G. W.; Schlegel, H. B.; Gill, P. M. W.; Johnson, B. G.; Robb, M. A.; Cheeseman, J. R.; Keith, T.; Peterson, G. A.; Montgomery, J. A.; Raghavachari, K.; Al-Laham, M. A.; Zakrzewski, V. G.; Ortiz, J. V.; Foresman, J. B.; Cioslowski, J.; Stefanow, B. B.; Nanayakkara, A.; Challacombe, M.; Peng, C. Y.; Ayala, P. Y.; Chen, W.; Wong, M. W.; Andres, J. L.; Replogle, E. S.; Gomperts, R.; Martin, R. L.; Fox, D. J.; Binkley, J. S.; Defrees, D. J.; Baker, J.; Stewart, J. J. P.; Head-Gordon, M.; Gonzalez, C.; Pople, J. A. Gaussian, Inc., Pittsburgh, PA, 1995.

(30) (a) NBO analysis: Reed, A. E.; Curtiss, L. A.; Weinhold, F. *Chem. Rev.* **1988**, 88, 899 and references cited therein. (b) NLMO bond orders: Reed, A. E.; Schleyer, P. v. R. *J. Am. Chem. Soc.* **1990**, 112, 1434. (c) NPA charges: Reed, A. E.; Weinstock, R. B.; Weinhold, F. *J. Chem. Phys.* **1985**, 83, 735.

Table 1. Total Energies (au) and Zero Point Energies ZPE (kcal/mol)^a

	PG	RHF/basis A	ZPE	MP2(full)/ basis A	Becke3LYP/ basis A	Becke3LYP/basis B// MP2(full)/basis A
CH ₂ CHOH	C _s	-152.894 69	38.2	-153.334 36	-153.814 34	-153.865 26
CH ₂ CHO ⁻	C _s	-152.311 15	28.4	-152.766 29	-153.244 06	-153.289 36
C ₆ H ₅ OH	C _s	-305.564 68	69.8	-306.518 73	-307.474 87	-307.558 22
C ₆ H ₅ O ⁻	C _{2v}	-304.991 81	61.0	-305.962 54	-306.915 47	-306.993 26
CH ₂ CHOLi	C _s	-159.806 45	31.1	-160.264 71	-160.785 83	-160.835 31
CH ₂ CHOLi	C ₁	-159.807 50	31.1	-160.265 23	-160.790 00	-160.837 16
CH ₂ CHONa	C _s	-314.185 99	30.2	-314.644 05	-315.540 22	-315.592 77
CH ₂ CHONa	C ₁	-314.189 43	30.2	-314.648 22	-315.546 08	-315.597 07
CH ₂ CHOK	C _s	-180.390 97	28.9	-181.029 42	-181.583 14	-181.628 09
CH ₂ CHOK	C ₁	-180.393 07	29.9	-181.034 53	-181.587 49	-181.632 16
CH ₂ CHORb	C _s	-176.146 93	29.7	-176.729 02	-177.356 26	-177.402 55
CH ₂ CHORb	C ₁	-176.149 30	29.8	-176.734 70	-177.360 43	-177.405 69
CH ₂ CHOCs	C _s	-172.207 22	29.7	-172.786 05	-173.428 83	-173.474 43
CH ₂ CHOCs	C ₁	-172.209 38	29.8	-172.791 64	-173.432 76	-173.477 33
C ₆ H ₅ OLi	C _{2v}	-312.481 70	63.4	-313.452 97	-314.448 75	-314.529 90
C ₆ H ₅ ONa	C _{2v}	-466.859 53	62.5	-467.832 68	-469.203 28	-469.287 78
C ₆ H ₅ OK	C _{2v}	-333.067 03	62.3	-334.218 14	-335.246 72	-335.324 35
C ₆ H ₅ ORb	C _{2v}	-328.823 11	62.1	-329.918 00	-331.020 06	-331.097 88
C ₆ H ₅ OCs	C _{2v}	-324.883 29	62.1	-325.975 11	-327.093 09	-327.171 63
H ₂ O	C _{2v}	-76.015 44	14.3	-76.206 94	-76.421 22	-76.458 35
OH ⁻	C _{∞v}	-75.375 07	2.9	-75.587 55	-75.795 37	-75.827 39
EtOH	C _s	-154.080 57	53.8	-154.531 47	-155.043 25	-155.094 88
EtO ⁻	C _s	-153.454 54	43.6	-153.924 25	-154.435 21	-154.482 64
LiOH	C _{∞v}	-82.913 36	8.4	-83.126 02	-83.380 90	-83.417 12
NaOH	C _{∞v}	-237.287 60	7.8	-237.500 93	-238.130 37	-238.168 59
KOH	C _{∞v}	-103.491 59	7.8	-103.886 05	-104.173 14	-104.203 70
RbOH	C _{∞v}	-99.246 54	7.7	-99.584 56	-99.945 00	-99.975 60
CsOH	C _{∞v}	-95.307 91	7.6	-95.642 29	-96.019 63	-96.052 08

^a Total energy in atomic units (au) (1 au = 627.5095 kcal/mol). Basis A: Li, Na, H, C, N, O, F (6-31+G*), K, Rb, Cs; 9VE-ECP MWB 6s6p2d/5s5p2d. Basis B: Li, Na, H, C, N, O, F (6-311++G**), K, Rb, Cs, 9VE-ECP MWB 6s6p2d/5s5p2d. ^b ZPE: zero point energy (kcal/mol) at the RHF/basis A level.

Table 2. Relative Energies of Bridged vs Linear Enolates (kcal/mol)^a

M	RHF/basis A	MP2(full)/basis A	Becke3LYP/ basis A	Becke3LYP/basis B// MP2(full)/basis A	Becke3LYP/basis B// MP2(full)/basis A + ΔZPE
Li	-0.7	-0.3	-2.6	-1.2	-1.2
Na	-2.2	-2.6	-4.2	-2.7	-2.7
K	-1.3	-3.2	-2.7	-2.6	-2.6
Rb	-1.2	-3.6	-2.6	-2.0	-1.9
Cs	-0.9	-3.5	-2.5	-1.8	-1.7

^a See footnotes in Table 1.

(GIAO-SCF/6-31+G*, NICS) were calculated with the MP2-(full)/basis A geometries, with Gaussian 94.

Results and Discussion

The allyl anion is the isoelectronic carbon equivalent of the enolate anion. The preferred *ab initio* geometries of the alkali allyl metals are bridged;^{18j} such structures also have been shown by isotopic perturbation,³² NMR,³³ and X-ray³⁴ studies. At MP2(full)/6-31G*/MP2(full)/6-31G*, the monomeric bridged lithium enolate structure is 5.1 kcal/mol more stable than the "linear" alternative.⁷ The preference for bridging in alkali enolates at more sophisticated levels of theory (see Table 2) is very small for lithium (1.2 kcal/mol)³⁵ and only modest for the other alkali metals (ranging from 2.7

(31) (a) Keith, T. A.; Bader, R. F. *Chem. Phys. Lett.* **1992**, *194*, 1. (b) Bader, R. F.; Keith, T. A. *J. Chem. Phys.* **1993**, *99*, 3683.

(32) (a) Saunders, M.; Telkowski, L.; Kates, K. R. *J. Am. Chem. Soc.* **1977**, *99*, 8070. (b) Faller, J. W.; Murray, H. H.; Saunders, M. *J. Am. Chem. Soc.* **1980**, *102*, 2306.

(33) (a) Winchester, W. R.; Bauer, W.; Schleyer, P. v. R. *J. Chem. Soc., Chem. Commun.* **1987**, 177. (b) Fraenkel, G.; Qiu, F. *J. Am. Chem. Soc.* **1996**, *118*, 5828.

(34) (a) Schumann, U.; Weiss, E.; Dietrich, H.; Mahdi, W. *J. Organomet. Chem.* **1987**, *229*, 332. (b) Boche, G.; Etzrodt, H.; Marsch, M.; Massa, W.; Baum, G.; Dietrich, H.; Mahdi, W. *Angew. Chem., Int. Ed. Engl.* **1986**, *25*, 104.

Table 3. Natural Charges of Vinyl Alcohol, the Nonbridged Alkali-Metal Acetaldehyde Enolates, and the Acetaldehyde Enolate Anion

M	C ₁	C ₂	O	M
H	0.239	-0.439	-0.598	0.371
Li	0.273	-0.656	-1.157	0.977
Na	0.292	-0.700	-1.120	0.990
K	0.301	-0.716	-1.108	0.994
Rb	0.304	-0.723	-1.100	0.995
Cs	0.302	-0.715	-1.106	0.991
anion	0.354	-0.865	-0.933	

Table 4. Natural Charges of the Bridged Alkali-Metal Acetaldehyde Enolates

M	C ₁	C ₂	O	M
Li	0.286	-0.839	-0.998	0.944
Na	0.322	-0.867	-0.982	0.963
K	0.315	-0.856	-0.987	0.979
Rb	0.316	-0.853	-0.987	0.982
Cs	0.303	-0.827	-0.995	0.974

kcal/mol for Na to 1.7 kcal/mol for Cs). Solvation and aggregation can easily overcome such small energy differences. Indeed, bridged alkali-metal enolate struc-

(35) The larger 5.1 kcal/mol energy difference between the bridged and linear form of the lithium acetaldehyde enolate at MP2(full)/6-31G*/MP2(full)/6-31G* reported earlier^{7a} stems from basis set superposition error (BSSE); diffuse function augmented basis sets are essential for the refined descriptions of polar organometallic systems.

Table 5. Geometries (Å, deg) of Vinyl Alcohol, the Nonbridged Alkali-Metal Acetaldehyde Enolates, and the Acetaldehyde Enolate Anion^a

M		C ₁ C ₂	C ₁ O	OM	MOC ₁	OC ₁ C ₂
H	RHF ^b	1.321 (1.318)	1.347 (1.340)	0.949	111.1	126.8 (126.9)
	RMP2	1.340	1.372	0.976	109.1	126.6
	B3LYP	1.337	1.366	0.972	109.8	127.0
Li	RHF ^b	1.337, 1.332	1.302, 1.296	1.618, 1.613	173.5 (175.2)	127.2 (127.2)
	RMP2	1.352	1.331	1.617	177.1	126.2
	B3LYP	1.351	1.321	1.623	176.8	126.9
Na	RHF ^b	1.344 (1.340)	1.293 (1.286)	1.983 (1.977)	168.9 (179.1)	127.9 (128.0)
	RMP2	1.357	1.323	1.981	173.6	127.0
	B3LYP	1.357	1.313	1.983	166.1	127.8
K	RHF ^b	1.347 (1.342)	1.290 (1.284)	2.300 (2.289)	168.0 (171.0)	128.1 (128.1)
	RMP2	1.360	1.321	2.284	172.2	127.3
	B3LYP	1.360	1.311	2.270	172.0	127.9
Rb	RHF ^b	1.348 (1.343)	1.288 (1.282)	2.456 (2.447)	167.1 (170.1)	128.2 (128.2)
	RMP2	1.362	1.320	2.441	171.2	127.4
	B3LYP	1.361	1.310	2.435	170.9	127.9
Cs	RHF ^b	1.347 (1.342)	1.290 (1.284)	2.561 (2.547)	165.4 (170.0)	128.1 (128.1)
	RMP2	1.360	1.323	2.535	170.9	127.2
	B3LYP	1.360	1.314	2.521	170.6	127.7
anion	RHF ^b	1.377 (1.372)	1.251 (1.244)			130.4 (130.4)
	RMP2	1.387	1.285			129.7
	B3LYP	1.389	1.274			130.2

^a See footnotes in Table 1. ^b Data from ref 7a are given in parentheses.

Table 6. Geometries (Å, deg) of the Bridged Acetaldehyde Enolates^a

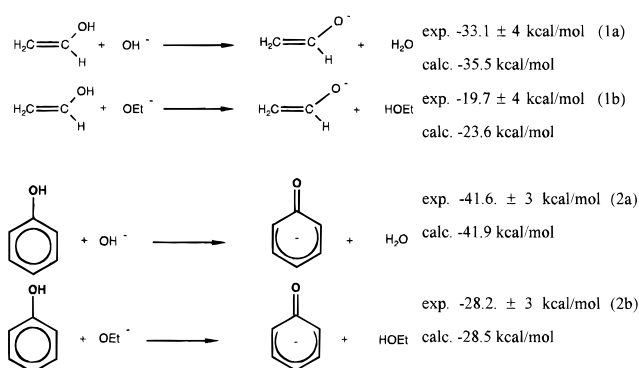
M		C ₁ C ₂	C ₁ O	OM	MOC ₂	OC ₂ C ₁
Li	RHF	1.365	1.281	1.750	87.0	124.4
	RMP2	1.379	1.313	1.755	84.4	124.0
	B3LYP	1.381	1.302	1.767	83.6	124.2
Na	RHF	1.370	1.271	2.124	91.4	126.5
	RMP2	1.383	1.303	2.156	88.3	126.4
	B3LYP	1.386	1.292	2.140	88.0	126.5
K	RHF	1.367	1.271	2.433	97.5	127.3
	RMP2	1.382	1.301	2.433	92.0	126.7
	B3LYP	1.382	1.292	2.425	92.8	127.0
Rb	RHF	1.367	1.270	2.588	99.2	127.6
	RMP2	1.382	1.300	2.586	93.5	127.0
	B3LYP	1.383	1.291	2.594	93.5	127.1
Cs	RHF	1.364	1.273	2.680	102.6	127.4
	RMP2	1.378	1.304	2.666	96.9	126.7
	B3LYP	1.377	1.296	2.648	98.6	127.1

^a See footnotes in Table 1.

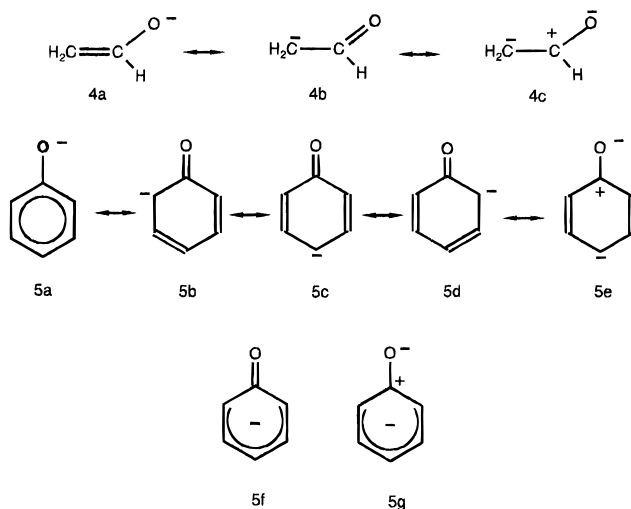
tures have not yet been observed experimentally, due to the strong tendency toward aggregation. The smaller tendency for bridging in alkali-metal enolates compared with allyl alkali-metal derivatives is a consequence of the much larger electronegativity of oxygen. In the bridged enolates, the negative charge on oxygen is smaller, and on C₂ larger, than in the linear isomers. In the allyl anions, in contrast, the negative charge is equally shared between C₁ and C₃.

As in our earlier study,^{7a} we have chosen the unbridged MOCH=CH₂ minima for our discussion on the charge localization due to the gegenion, as these model the M-O interactions found in the crystal structures as well as those expected in solution (lithium acetaldehyde enolate forms a tetrameric aggregate in THF solution).³⁶ The experimental stabilization energies of the enolate anion (eq 1) and of the phenoxide anion (eq 2) are very large.³⁷ Our *ab initio* Becke3LYP/basis B//MP2(full)/basis A energies, corrected to 298 K, are within the experimental error limits.

The negative charges are delocalized both in the enolate (**4**) and the phenolate (**5**) anions. The conven-



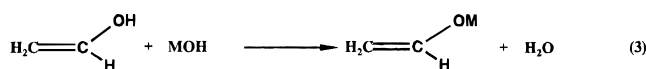
tional representations employ resonance structures **4a,b** and **5a–d**, but ionic contributions **4c** and **5e** also are



important. In fact, considering the geometry, **5f** or **5g** (rather than **5a**) may be the best single depiction of the phenolate anion (this conclusion is reinforced in the later discussion). In a very recent *ab initio* study on the origin of the acidity in enols and carbocyclic acids, Wiberg, Ochterski, and Streitwieser analyzed the changes in electron population resulting from deprotonation of vinyl alcohol.³⁸ On formation of the anion, not only is

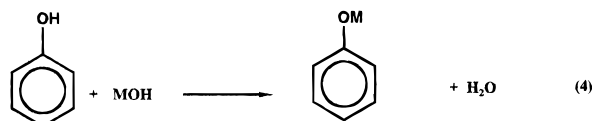
(36) Wen, J. Q.; Grutzner, J. B. *J. Org. Chem.* **1986**, *51*, 4220.

(37) Lias, S. G.; Bartmess, J. E.; Liebmann, J. F.; Holmes, J. L.; Levin, R. D.; Mallard, W. G. *J. Phys. Chem. Ref. Data* **1988**, *17*, Suppl. 1.

Table 7. Energies of Eq 3 (kcal/mol)^a

M	RHF/basis A	MP2(full)/basis A	Becke3LYP/basis A	Becke3LYP/basis B// MP2(full)/basis A	Becke3LYP/basis B// MP2(full)/basis A +ΔZPE	exptl ^b
Li	-8.7	-7.1	-7.4	-7.1	-8.2	
Na	-12.0	-9.9	-10.5	-10.8	-12.2	
K	-12.6	-10.0	-10.6	-11.0	-13.5	
Rb	-13.3	-10.7	-11.4	-12.6	-14.3	
Cs	-12.6	-10.3	-10.1	-9.7	-11.3	
anion	-35.7	-32.2	-34.9	-34.6	-34.9 (-35.5) ^c	-33.1 ± 4

^a See footnotes in Table 1. ^b Reference 37 (298 K). ^c Corrected to 298 K.

Table 8. Energies of Eq 4 (kcal/mol)^a

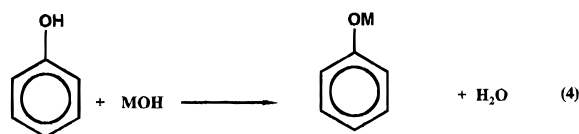
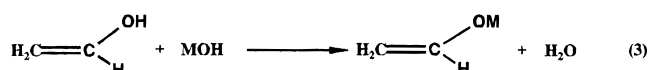
M	RHF/basis A	MP2(full)/basis A	Becke3LYP/basis A	Becke3LYP/basis B// MP2(full)/basis A	Becke3LYP/basis B// MP2(full)/basis A +ΔZPE	exptl ^b
Li	-12.0	-9.5	-8.9	-8.1	-8.6	
Na	-14.2	-12.5	-12.1	-12.1	-12.9	
K	-16.4	-12.7	-12.5	-13.0	-14.0	
Rb	-17.2	-13.6	-13.4	-14.1	-15.1	
Cs	-16.4	-13.2	-12.4	-12.4	-13.3	
anion	-42.4	-39.7	-41.7	-41.4	-40.9 (-41.9) ^c	-41.6 ± 4

^a See footnotes in Table 1. ^b Reference 37 (298 K). ^c Corrected to 298 K.

the σ electron density formerly associated with the proton donated to the oxygen but the π density at the oxygen also is transferred to the C–C double bond. The negative charge on oxygen repels both the σ and the π electrons of the adjacent carbon and polarizes the double bond. These results emphasize the importance of resonance contribution **4c** to the stabilization of the enolate anion. The more extensive delocalization of the negative charge in phenoxides accompanied with the greater polarizability of the larger phenyl group results in the greater acidity of phenol than vinyl alcohol (the experimental gas-phase acidities ΔH_{acid} (298 K) are 350.2 ± 2.5 kcal/mol for phenol and 357.7 ± 3 kcal/mol for vinyl alcohol).³⁷ The corresponding *ab initio* Becke3LYP/basis B//MP2(full)/basis A acidities (corrected to 298 K: phenol, 345.0 kcal/mol; vinyl alcohol, 351.5 kcal/mol) are just outside the experimental error limits, but the experimental and computed energy differences agree well.

Truly “free” anions only exist in the gas phase. Syntheses with polar organometallics generally are carried out in ether solvents like THF or in hexane in the presence of ligands like TMEDA.³⁹ Under these conditions, dimeric, tetrameric or even hexameric aggregates are formed,^{12–16} and the role of the metal is important.^{1–7} As pointed out in the Introduction, charge localizing due to the gegenion reduces the stabilization energies both of enolates (eq 3)^{7a} and of phenolates (eq 4) dramatically.

While the metalation energies for eqs 3 and 4 (see Tables 7 and 8) are much less exothermic than eqs 1a



and 2a, the difference between enolates and phenolates with the same alkali metal is rather small. The energies of eqs 3 and 4 are smallest for the lithium compounds (–8.2 kcal/mol for enolate and –8.6 kcal/mol for the phenolate); the increases for the other alkali metals (to 14 or 15 kcal/mol) are only modest. The considerably larger stabilization energies for the free anions emphasizes that the presence of the metal cation in a contact ion pair counteracts the stabilization of the free anion.⁶

All the metal ions (compare Tables 3, 4, and 9) have near unit natural charges³⁰ (+0.977 to +0.995); these are nearly the same for each metal in both the phenolates and the enolates. The lithium charge is only slightly less that of the other alkali metals. Thus, all the M–O bonds are essentially completely ionic. The electrostatic charge localizing effect of the metals is responsible for the higher oxygen charges in the ion-paired species compared to the free anions.^{7a}

Geometries. The geometries of the optimized molecules are given in Tables 5, 6, and 10. The influence of the metal gegenion is evident, as is the effect of electron correlation (MP2 and B3LYP vs HF). The C₁C₂ bond is shortest in vinyl alcohol and longest in the free enolate anion. The values for the metalated compounds are intermediate.⁷ The same is true for the C₁C₂

(38) Wiberg, K. B.; Ochterski, J.; Streitwieser, A. *J. Am. Chem. Soc.* **1996**, *118*, 8291.

(39) (a) Brandsma, L.; Verkruijse, H. *Preparative Polar Organometallic Chemistry 1*; Springer: Berlin, 1987. (b) Brandsma, L. *Preparative Polar Organometallic Chemistry 2*; Springer: Berlin, 1990.

Table 9. NPA Charges of Phenol, the Phenolate Anion, and the Alkali-Metal Phenolates

M	C ₁	C ₂	C ₃	C ₄	C ₅	C ₆	O	M
H	0.375	-0.299	-0.195	-0.284	-0.195	-0.333	-0.767	0.508
Li	0.434	-0.340	-0.201	-0.321	-0.201	-0.340	-1.137	0.978
Na	0.449	-0.355	-0.199	-0.337	-0.199	-0.335	-1.100	0.992
K	0.457	-0.360	-0.199	-0.343	-0.199	-0.360	-1.087	0.995
Rb	0.460	-0.363	-0.199	-0.346	-0.199	-0.363	-1.080	0.996
Cs	0.458	-0.360	-0.199	-0.343	-0.199	-0.360	-1.087	0.992
anion	0.499	-0.401	-0.204	-0.418	-0.204	-0.401	-0.904	

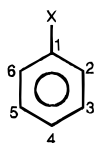
Table 10. Geometries (Å, deg) of the Phenolates^a

M	PG	C ₁ C ₂	C ₂ C ₃	C ₃ C ₄	C ₄ C ₅	C ₅ C ₆	C ₆ C ₁	C ₁ O	OM	C ₁ C ₂ C ₃	C ₂ C ₃ C ₄	C ₃ C ₄ C ₅	C ₄ C ₅ C ₆	C ₅ C ₆ C ₁	C ₆ C ₁ C ₂	OC ₁ C ₂	
H	C _s	RHF	1.389	1.384	1.391	1.385	1.389	1.387	1.353	0.948	119.6	120.8	119.1	120.6	119.7	120.2	117.4
		RMP2	1.398	1.396	1.400	1.397	1.399	1.398	1.379	0.975	119.5	120.6	119.4	120.5	119.6	120.4	116.8
		B3LYP	1.399	1.395	1.400	1.397	1.398	1.399	1.373	0.970	119.5	120.7	119.4	120.5	119.7	120.3	117.2
Li	C _{2v}	RHF	1.404	1.385	1.389	1.389	1.385	1.404	1.305	1.617	121.0	121.1	118.4	121.1	121.0	117.4	121.3
		RMP2	1.411	1.397	1.399	1.399	1.397	1.411	1.334	1.620	121.0	120.7	118.9	120.7	121.0	117.8	121.1
		B3LYP	1.415	1.396	1.400	1.400	1.396	1.415	1.325	1.620	121.0	120.8	118.7	120.8	121.0	117.6	121.2
Na	C _{2v}	RHF	1.410	1.384	1.390	1.390	1.384	1.410	1.296	1.982	121.4	121.2	118.1	121.2	121.4	116.6	121.7
		RMP2	1.416	1.397	1.400	1.400	1.397	1.416	1.326	1.984	121.5	120.7	118.7	120.7	121.5	116.9	121.6
		B3LYP	1.420	1.396	1.401	1.401	1.396	1.420	1.317	1.975	121.4	121.0	118.5	121.0	121.4	116.8	121.6
K	C _{2v}	RHF	1.412	1.384	1.391	1.391	1.384	1.412	1.296	1.982	121.5	121.3	118.0	121.3	121.5	116.3	121.8
		RMP2	1.418	1.397	1.400	1.400	1.397	1.418	1.325	2.286	121.7	120.8	118.6	120.8	121.7	116.5	121.7
		B3LYP	1.423	1.395	1.401	1.401	1.395	1.423	1.315	2.256	121.6	121.0	118.4	121.0	121.6	116.4	121.8
Rb	C _{2v}	RHF	1.413	1.384	1.391	1.391	1.384	1.413	1.292	2.456	121.6	121.3	118.0	121.3	121.6	116.2	121.9
		RMP2	1.419	1.397	1.400	1.400	1.397	1.419	1.324	2.442	121.7	120.8	118.6	120.8	121.7	116.4	121.8
		B3LYP	1.424	1.395	1.402	1.402	1.395	1.424	1.313	2.427	121.7	121.0	118.4	121.0	121.7	116.2	121.9
Cs	C _{2v}	RHF	1.412	1.384	1.391	1.391	1.384	1.412	1.294	2.563	121.5	121.3	118.0	121.3	121.5	116.3	121.9
		RMP2	1.418	1.397	1.400	1.400	1.397	1.418	1.327	2.536	121.6	120.8	118.6	120.8	121.6	116.5	121.7
		B3LYP	1.422	1.395	1.401	1.401	1.395	1.422	1.317	2.518	121.5	121.0	118.4	121.0	121.5	116.5	121.8
anion	C _{2v}	RHF	1.439	1.379	1.397	1.397	1.379	1.439	1.252		122.3	122.1	117.1	122.1	122.3	114.1	123.0

^a See footnotes in Table 1.

distances in the corresponding phenolates, although the C₁C₂ distance is longer than in the enolates. Electron correlation, both at MP2 and Becke3LYP density functional levels, results in longer C–C and C–O distances compared to the HF results. The M–O bond distances in Li and Na compounds are nearly unaffected by electron correlation. For the heavier alkali metals (K–Cs), correlation reduces the M–O distances slightly (see Tables 5, 6, and 10). Since the potential energy surfaces, especially for the heavier alkali metals, are very flat and the distances are large, the differences are insignificant.

Substituents result in small, characteristic changes of the benzene geometry.^{40–44} The C₆C₁C₂ angle (α)



at the ipso position is most sensitive, varying, e.g. from about 112° for C₆H₅Li to about 125° for C₆H₅N₂⁺.⁴⁴ For the phenolates, α is smallest in the free phenolate anion

(40) Domenicano, A. In *Accurate Molecular Structures*; Domenicano, A., Hargittai, I., Eds.; Oxford University Press: New York, 1992; pp 482–488 and references cited.

(41) Keidel, F. A.; Bauer, S. H. *J. Chem. Phys.* **1956**, *25*, 1218.

(42) (a) Nygaard, L.; Bojesen, I.; Pedersen, T.; Rastrup-Andersen, J. *J. Mol. Struct.* **1968**, *2*, 209. (b) Casado, J.; Nygaard, L.; Sørensen, G. O. *J. Mol. Struct.* **1971**, *8*, 211. (c) Lister, D. G.; Tyler, J. K.; Høg, J. H.; Larsen, N. W. *J. Mol. Struct.* **1974**, *23*, 253. (d) Cox, A. P.; Ewart, I. C.; Stigliani, W. M.; *J. Chem. Soc., Faraday Trans. 2* **1975**, *71*, 504. (e) Michel, F.; Nery, H.; Nosberger, P.; Roussy, G. *J. Mol. Struct.* **1976**, *30*, 409. (f) Larsen, N. W. *J. Mol. Struct.* **1979**, *51*, 175. (g) Amir-Ebrahimi, V.; Choplin, A.; Demaison, J.; Roussy, G. *J. Mol. Struct.* **1981**, *89*, 42.

(43) (a) Bock, C. W.; Trachtman, M.; George, P. *J. Mol. Struct. (Theochem)* **1985**, *122*, 155. (b) Bock, C. W.; Trachtman, M.; George, P. *J. Comput. Chem.* **1985**, *6*, 592.

Table 11. Natural Charges and Ipso Angle α in Lithium Phenolate as a Function of the Li–O Distance

$d(\text{Li–O})$ (Å)	O	M	α
1.617	-1.137	0.978	117.4
2.0	-1.093	0.982	116.9
3.0	-1.015	0.991	115.7
4.0	-0.968	0.997	115.1
5.0	-0.942	0.999	114.7
6.0	-0.926	0.999	114.6
7.0	-0.916	1.000	114.5
8.0	-0.909	1.000	114.4
∞	-0.904	1.000	114.1

(114.0°, $Q(\text{C}_1) = 0.499$) and largest for phenol (120.3; $Q(\text{C}_1) = 0.375$). The angles of metalated compounds are intermediate, ranging from 117.6° (M = Li, $Q(\text{C}_1) = 0.434$) to 116.2° (M = Rb, $Q(\text{C}_1) = 0.460$). Indeed, the bond angle α is related to the charge on C₁ (see Tables 9 and 10).

The charge localizing influence is still very effective for long M–O distances, since electrostatic interaction energies decrease with the inverse of the distance, r^{-1} . As a demonstration, we optimized lithium phenolate with Li–O distances fixed from 2–8 Å using RHF basis A and compared the lithium and oxygen charges as well as α with the free phenolate anion and also with the completely optimized lithium phenolate ($d(\text{Li–O}) = 1.617$ Å, see Table 11). Even at a Li–O separation of 4 Å, the charge on oxygen is increased (-0.968 vs -0.904) and the bond angle α widened (115.1 vs 114.1) with respect to the free phenolate anion. This suggests that

(44) (a) Domenicano, A.; Vaciago, A.; Coulson, C. A. *Acta Crystallogr.* **1975**, *B31*, 221. (b) Domenicano, A.; Vaciago, A.; Coulson, C. A. *Acta Crystallogr.* **1975**, *B31*, 1630. (c) Domenicano, A.; Vaciago, A. *Acta Crystallogr.* **1979**, *B35*, 1382. (d) Domenicano, A.; Murray-Rust, P.; Vaciago, A. *Acta Crystallogr.* **1983**, *B39*, 457. (e) Dunitz, J. D.; Wallis, J. D. *Helv. Chim. Acta* **1984**, *67*, 1374.

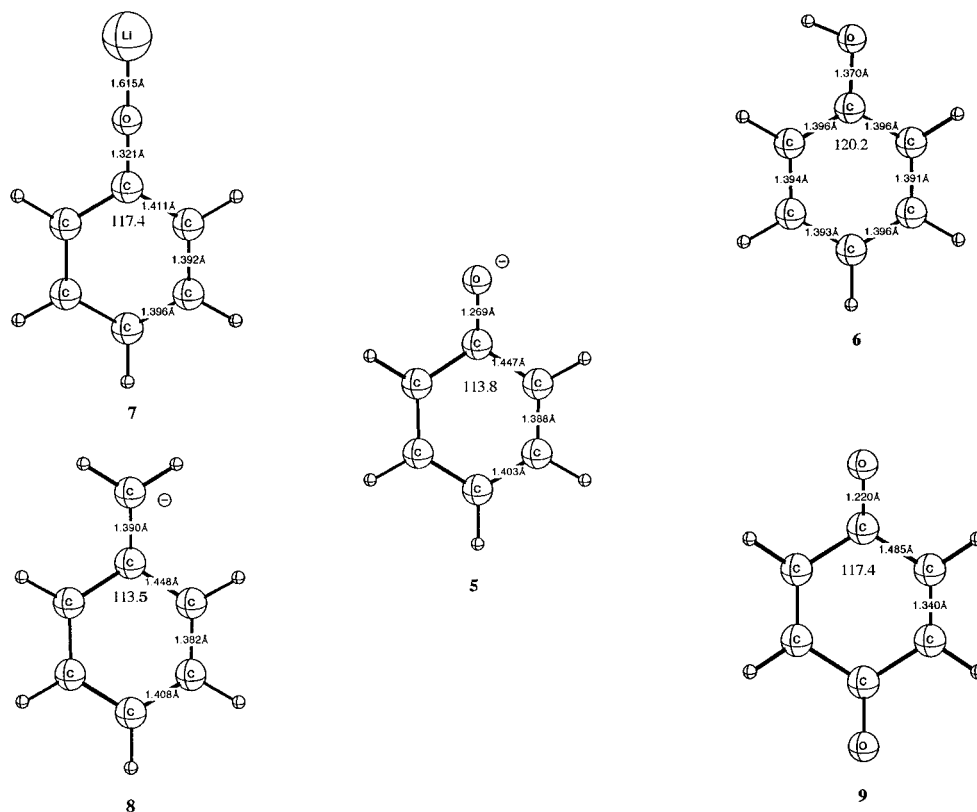


Figure 1. Becke3LYP/6-311+G**.

counterion effects also are important in solvent-separated ion pairs.

Structure of the Phenolate Anion and Its Aromaticity. The structures of the phenolate anion (**5**), phenol (**6**), and lithium phenolate (**7**), as well as the comparison molecules, the benzyl anion (**8**) and *p*-benzoquinone (**9**), optimized at Becke3LYP/6-311+G** are depicted in Figure 1. Bond length equalization due to cyclic delocalization is the geometric criterion of aromaticity.^{20,45–47} The C–C bond lengths in aromatic hydrocarbons are compared with one another and with the benzene value (ca. 1.40 Å). The bond lengths reveal the extent of electron delocalization in molecules.^{20,45–47} Whereas the C–C bond lengths are within 0.005 Å in phenol (**6**), the C–C lengths differ by 0.019 Å in the ion-paired lithium phenolate structure (**7**). In contrast, the *p*- π delocalization of the free phenolate ion (**5**) causes a much more substantial bond alternation (0.059 Å) in the benzene ring. The variation in the CC lengths of *para*-benzoquinone (**9**, $\Delta r = 0.145$ Å) is much larger. Hence, the phenolate anion (**5**) has about 63% of the aromatic character of phenol (**6**) on this basis. The C–O distance in **5** (1.269 Å, computed at Becke3LYP/6-311+G**) is closer to that in *para*-benzoquinone (**9**, 1.220 Å) than in phenol (**6**, 1.370 Å). However, the C–O[−] distance in alcoholates (e.g. 1.335 Å in CH₃O[−]) are generally shorter than in alcohols (e.g. 1.423 Å in CH₃OH). Hence, the depiction of the phenolate ion, considering the geometry, might well be the “quinoid” structure **5f**. Since the charges on oxygen (−0.90) and on the ipso carbon

(+0.50) are both large, **5g** contributes substantially. Similar bond alternation in the benzyl anion (**8**), the isoelectronic carbon equivalent to the phenolate anion, has been described by Dorigo, Li, and Houk.⁴⁸ Remarkably, the ring geometries of the benzyl and the phenolate anions are nearly identical (see Figure 1).

Magnetic Properties. The experimental³⁶ ¹³C chemical shifts are in good agreement with the calculated ¹³C chemical shifts of the linear lithium enolates but are completely different from the calculated shifts for the bridged enolates (Tables 12 and 13). This (and other evidence) suggests that bridged alkali-metal enolates do not exist in THF solution. Ion-pairing changes the charge distribution and the shieldings of all the atoms in enolates, especially for C₂. Whereas C₂ is relatively shielded in the free enolate anion ($\delta(^{13}\text{C}) = 51.3$ ppm), ion pairing results in deshielding (for M = Li, $\delta(^{13}\text{C}) = 80.0$ ppm) even at longer M–O distances ($\delta(^{13}\text{C}) = 71.8$ ppm for M = Cs). The $\delta(^{13}\text{C})$ differences at C₁ are less pronounced but still are significant (see Table 13).

In the phenolates, C₁ and C₄ are the most affected by ion pairing. The calculated shifts (Table 12) on C₁ vary from 166.5 ppm for lithium to 182.3 ppm for the free anion. The deshielding of C₄ in the ion-paired structures is also evident: $\delta(^{13}\text{C}) = 110.6$ ppm with Li but 91.5 ppm for the free anion. In contrast, the C₂ and C₃ shifts in phenol, the alkali phenolates, and the free phenolate anion are nearly the same, varying less than 2 ppm.

There is a renewed interest in using magnetic properties as aromaticity criteria.^{19,20,45} The proton chemical shifts of benzenoid aromatics have long been employed

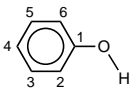
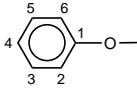
(45) Schleyer, P. v. R.; Freeman, P. K.; Jiao, H.; Goldfuss, B. *Angew. Chem., Int. Ed. Engl.* **1995**, *34*, 237.

(46) Minkin, V. J.; Glukhovtsev, M. N.; Simkin, B. Y. *Aromaticity and Antiaromaticity; Electronic and Structural Aspects*; Wiley: New York, 1994.

(47) (a) Julg, A.; Francois, P. *Theor. Chim. Acta* **1967**, *7*, 249. (b) van der Kerk, M. S. *J. Organomet. Chem.* **1981**, *215*, 315.

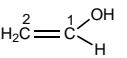
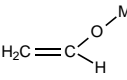
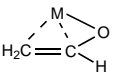
(48) Dorigo, A. E.; Li, Y.; Houk, K. N. *J. Am. Chem. Soc.* **1989**, *111*, 6942.

Table 12. GIAO-SCF (Basis A) Calculated ^1H and ^{13}C Chemical Shifts (δ , ppm Relative to TMS = 0.0 ppm) on the MP2(Full)/Basis A Optimized Geometries^a

molecule		C ₁	C ₂	C ₃	C ₄	C ₅	C ₆	H(C ₂)	H(C ₃)	H(C ₄)	H(C ₅)	H(C ₆)	H(OH)
	calc	155.7	110.5	131.3	118.1	132.8	115.2	6.7	7.6	7.1	7.8	7.4	4.2
	exptl ^b	155.1	115.7	130.1	121.4	130.1	115.7	6.7	7.1	6.8	7.1	6.8	
M = Li	exptl ^c	166.5	116.7	131.7	110.6	131.7	116.7	6.9	7.5	6.5	7.5	6.9	
M = Na		167.8	119.9	128.4	114.5	128.4	119.9						
M = K		171.0	116.0	132.1	107.7	132.1	116.0	6.7	7.4	6.3	7.4	6.7	
M = Rb		179.7	115.1	132.2	106.4	132.2	115.1	6.6	7.2	6.1	7.2	6.6	
M = Cs		179.9	115.9	132.5	106.2	132.5	115.9	7.2	7.5	6.3	7.5	7.2	
M = Cs		178.9	116.0	132.1	106.9	132.1	116.0	7.4	7.6	6.4	7.6	6.4	
M = -		182.3	115.4	131.7	91.5	131.7	115.4	6.3	7.0	5.1	7.0	6.3	

^a See Table 1 for details. ^b Reference 51. ^c Reference 13h (THF, -80 °C).

Table 13. GIAO-SCF (Basis A) Calculated ^1H and ^{13}C Chemical Shifts (δ , ppm Relative to TMS = 0.0 ppm) on the MP2(full)/Basis A Optimized Geometries^a

molecule		C ₁	C ₂	H(C ₁)	H(C ₂)	H(C ₂)	H(OH)
	calc	151.0	84.6	6.9	4.2	4.0	4.1
	calc	160.0	80.0	7.4	3.9	3.2	
M = Li	exptl ^b	158.0	81.0				
M = Na		163.9	73.8	7.5	3.5	2.9	
M = K		166.2	71.6	7.6	3.5	2.8	
M = Rb		166.9	70.6	7.6	3.4	2.7	
M = Cs		166.8	71.8	7.7	3.5	2.8	
M = -		176.5	51.3	8.4	2.7	1.5	
							
M = Li		179.6	64.9	8.6	3.1	3.2	
M = Na		183.9	58.6	8.7	2.6	2.9	
M = K		180.0	62.1	8.1	2.6	2.7	
M = Rb		179.3	62.8	8.1	2.5	2.5	
M = Cs		175.5	67.3	8.0	2.6	2.8	

^a See Table 1 for details. ^b Reference 36 (1.2 M, -86 °C, THF).

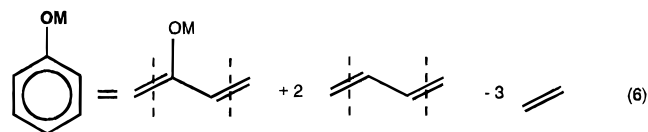
for this purpose,⁴⁹ although the paratropic ring current effects on the outside of rings are relatively small.⁵⁰ The capability of the newer quantum chemical programs²⁹ to compute various magnetic properties facilitates their wider application.

In particular, magnetic shieldings can be computed, *e.g.* at the center of rings, where the diatropic effects are quite large.¹⁹ Our NICS aromaticity criterion¹⁹ is based on such computed absolute shieldings, with the sign reversed to confirm to the experimental NMR chemical shift conventions (minus = upfield). The NICS(0) for benzene, -9.72 (Table 14), may be thought of as the chemical shift of a hypothetical noninteracting atom in the center of the ring. Table 13 also includes NICS(*n*) data, *i.e.* computed at arbitrary points *n* Å above the ring centers. These NICS (*n*) values are typically larger than NICS(0) (due to the paratropic local

shielding effects of the σ CC and CH bonds in the ring plane)⁵¹ but generally are parallel in behavior. Consequently, only the NICS(0) values, simply called "NICS" are discussed.

To what extent does ion pairing influence the aromaticity of phenolates? The results of our NICS¹⁹ calculations are summarized in Table 14. The phenol NICS (-10.83) is greater than the benzene NICS (-9.72). The free phenolate anion NICS is much less (-6.25, or about 58% of the phenol value), which can be rationalized by the reduction of aromaticity due to the predominance of the quinonoid structures **5f** or **5g**. Ion pairing due to the gegenion reduces such charge distribution; resonance structures **5b-e** are less important in the metalated phenolates. The NICS values of the alkali phenolates increase down the group from Li to Cs as the O-M distance increases; nevertheless, the charge localization effect is still very effective for cesium.

In addition to NICS, we also evaluated other magnetic criteria of aromaticity,²⁰ *e.g.* the diamagnetic susceptibility exaltation (Λ , ppm cgs)²² and the diamagnetic susceptibility anisotropy (χ_{anis} , ppm cgs)²³ to assess the aromaticity of phenol, the phenolate anion, and lithium phenolate. Λ , the only measurable property which is uniquely associated with aromaticity,²¹ is defined as the difference between the bulk magnetic susceptibility (χ_{M}) of a compound and the susceptibility (χ_{M}) estimated from an increment system for the same structure without cyclic delocalization ($\Lambda = \chi_{\text{M}} - \chi_{\text{M}}$).^{22c} In this paper, Λ is derived from the homodesmotic eq 6 using the CSGT data.³¹



The reduced aromaticity of the free phenolate anion also is demonstrated by the smaller magnetic susceptibility exaltation of $\Lambda = -9.1$, only 59% of $\Lambda = -15.5$ for phenol (see Table 15). Ion pairing increases the magnetic susceptibility exaltation for lithium phenolate ($\Lambda = -14.4$) relative to the free anion. Hence, phenol and the ion-paired alkali-metal phenolates have more

(49) (a) Pople, J. A. *J. Chem. Phys.* **1956**, *24*, 1111. (b) Jackman, L. M.; Sondheimer, F.; Amiel, Y.; Ben-Efraim, D. A.; Gaoni, Y.; Wolovsky, R.; Bother-By, A. A. *J. Am. Chem. Soc.* **1962**, *84*, 4307. (c) Oth, J. F. M.; Woo, E. P.; Sondheimer, F. *J. Am. Chem. Soc.* **1973**, *95*, 7337. (d) Sorensen, T. S.; Whitworth, S. M. *J. Am. Chem. Soc.* **1990**, *112*, 8135.

(50) (a) Pople, J. A.; Untch, K. G. *J. Am. Chem. Soc.* **1966**, *88*, 4811. (b) Sondheimer, F. *Acc. Chem. Res.* **1972**, *5*, 81.

(51) Waugh, J. S.; Fessenden, R. W. *J. Am. Chem. Soc.* **1957**, *79*, 846.

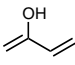
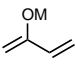
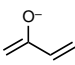
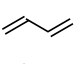
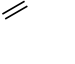
(52) Hesse, M.; Meier, H.; Zeeh, B. *Spektroskopische Methoden in der organischen Chemie*; Thieme Verlag: Stuttgart, Germany, 1984.

Table 14. GIAO-SCF (Basis A) Calculated Nucleus-Independent Chemical Shifts (NICS)^a on the MP2(full)/Basis A Optimized Geometries^b

molecule	NICS(0) ^c	NICS(0.5)	NICS(1)	NICS(1.5)	NICS(2)	NICS(2.5)	NICS(3)
C ₆ H ₆	-9.72	-11.54	-11.54	-8.39	-5.33	-3.36	-2.18
C ₆ H ₅ OH	-10.83	-11.99	-11.26	-7.97	-4.99	-3.11	-2.01
C ₆ H ₅ OLi	-9.91	-10.80	-10.31	-7.36	-4.64	-2.90	-1.88
C ₆ H ₅ ONa	-9.15	-10.38	-9.98	-7.15	-4.51	-2.83	-1.84
C ₆ H ₅ OK	-8.80	-10.19	-10.05	-7.31	-4.67	-2.98	-1.97
C ₆ H ₅ ORb	-7.95	-9.32	-9.19	-6.52	-3.98	-2.38	-1.46
C ₆ H ₅ OCs	-7.53	-8.90	-8.76	-6.11	-3.61	-2.06	-1.18
C ₆ H ₅ O ⁻	-6.25	-7.51	-7.60	-5.53	-2.24	-1.48	-1.01

^a See ref 19. ^b See Table 1 for details. ^c NICS(*n*): NICS computed *n* Å above the ring center.

Table 15. Becke3LYP/6-31G* Computed Magnetic Susceptibilities Exaltations (Λ) and Anisotropies (χ_{anis}) (ppm cgs)

molecule	χ _{tot}	Λ	χ _{anis}
C ₆ H ₅ OH	-52.5	-15.5	-62.0
C ₆ H ₅ O ⁻	-47.5	-9.1	-45.7
C ₆ H ₅ OLi	-52.5	-14.4	-58.8
C ₆ H ₆	-46.1	-16.7	-69.6
	-30.4		-13.1
	-31.5		-15.3
	-31.8		-13.5
	-22.8		-17.4
	-13.0		-9.6

aromatic character than the phenolate anion. The computed anisotropies χ_{anis} for the molecules 5–7 (see Table 15) follow the same trend as the other criteria of aromaticity (Λ, NICS) which indicate that the phenolate anion has only about 60% of the aromaticity of phenol.

Conclusion

Ion-pair interactions influence the geometries, the charge distributions, the ¹³C chemical shifts, and other

magnetic properties, as well as the reaction energies of alkali-metal enolates and phenolates, but do so to similar extents. Hence, phenolates are suitable as models for enolates. The presence of an alkali-metal cation counteracts much of the stabilization of the free anion. The charge-localizing effect is still effective at long M–O distances, since electrostatic interaction energies decrease only with the inverse of the distance. The geometry and electronic structure of the free phenolate anion indicate the importance of quinoid resonance structure **5f** or **5g**. The conventional representation **5a** is misleading in this sense. The p-π delocalization in the free anion reduces the aromatic character to about 60% of that of phenol (based on geometrical and magnetic criteria), but the aromaticity is largely restored in the alkali-metal ion pairs due to the charge-localizing effect of the positive counterions.

Acknowledgment. This work was supported by the Deutsche Forschungsgemeinschaft, the Fonds der Chemischen Industrie, the Volkswagen Stiftung, and the Convex Computer Cooperation. We thank Dr. Haijun Jiao for his advice concerning the NICS calculations.

OM960763O